

# Characterization of the first microRNA in human *CDH1* that affects cell cycle and apoptosis and indicates breast cancers progression

Sedigheh Gharbi<sup>1</sup> | Zahra Mohammadi<sup>1</sup> | Maryam Saedi Dezaki<sup>1</sup> |  
Sadat Dokanehiifard<sup>2</sup> | Shahriar Dabiri<sup>3</sup> | Eberhard Korsching<sup>4</sup> 

<sup>1</sup>Department of Biology, Faculty of Sciences, Shahid Bahonar University of Kerman, Kerman, Iran

<sup>2</sup>Department of Human Genetics, Sylvester Comprehensive Cancer Center, University of Miami Miller School of Medicine, Miami, Florida, USA

<sup>3</sup>Department of Pathology, Pathology and Stem Cell Research Center, Kerman University of Medical Sciences, Kerman, Iran

<sup>4</sup>Institute of Bioinformatics, Faculty of Medicine, University of Münster, Münster, Germany

## Correspondence

Eberhard Korsching, Institute of Bioinformatics, Faculty of Medicine, University of Münster, Niels-Stensen-St 14, Münster, 48149, Germany.  
Email: eberhard.korsching@uni-muenster.de

## Funding information

Kerman University of Medical Sciences, Grant/Award Number: 96000216; Westfälische Wilhelms-Universität Münster, Grant/Award Number: Open Access Publication Fund

## Abstract

The E-cadherin protein (Cadherin 1, gene: *CDH1*), a master regulator of the human epithelial homeostasis, contributes to the epithelial-mesenchymal transition (EMT) which confers cell migratory features to the cells. The EMT is central to many pathophysiological changes in cancer. Therefore, a better understanding of this regulatory scenario is beneficial for therapeutic regimens. The *CDH1* gene is approximately 100 kbp long and consists of 16 exons with a relatively large second intron. Since none microRNA (miRNA) has been identified in *CDH1* up to now we screened the *CDH1* gene for promising miRNA hairpin structures in silico. Out of the 27 hairpin structures we identified, one stable RNA fold with a promising sequence motive was selected for experimental verification. The exogenous validation of the hairpin sequence was performed by transfection of HEK293T cells and the mature miRNA sequences could be verified by quantitative polymerase chain reaction. The endogenous expression of the mature miRNA provisionally named CDH1-i2-miR-1 could be confirmed in two normal (HEK293T, HUVEK) and five cancer cell lines (MCF7, MDA-MB-231, SW480, HT-29, A549). The functional characterization by the 3-(4,5-dimethylthiazol-2-yl)-2,5-diphenyltetrazolium bromide assay showed a suppression of HEK293T cell proliferation. A flow cytometry-based approach showed the ability of CDH1-i2-miR-1 to arrest transfected cells on a G2/M state while annexin staining exemplified an apoptotic effect. BAX and PTEN expression levels were affected following the overexpression with the new miRNA. The in vivo expression level was assessed in 35 breast tumor tissues and their paired nonmalignant marginal part. A fourfold downregulation in the tumor specimens compared to their marginal controls could be observed. It can be concluded that the sequence of the

Sedigheh Gharbi and Zahra Mohammadi contributed equally to this study.

This is an open access article under the terms of the Creative Commons Attribution-NonCommercial-NoDerivs License, which permits use and distribution in any medium, provided the original work is properly cited, the use is non-commercial and no modifications or adaptations are made.

© 2022 The Authors. *Journal of Cellular Biochemistry* published by Wiley Periodicals LLC

hub gene *CDH1* harbors at least one miRNA but eventually even more relevant for the pathophysiology of breast cancer.

#### KEYWORDS

apoptosis, bioinformatics, breast cancer, Cadherin 1, E-cadherin, epithelial-mesenchymal transition, microRNA prediction

## 1 | INTRODUCTION

The human E-cadherin (Cadherin 1, gene: *CDH1*), also known as epithelial cadherin, is a member of the cadherin superfamily, which is composed of more than 110 family members and is a core component of the epithelial homeostasis.<sup>1,2</sup> In epithelial cells, Cadherin 1 is a key regulator to form the adherence junctions and its developmental role starts early on a two-cell stage.<sup>3,4</sup> In cancer, a downregulation of Cadherin 1 expression is associated with cell invasion, tumor progression, metastasis, and increased proliferation, especially in tumors of epithelial origin such as carcinomas and melanomas.<sup>5,6</sup> These physiological processes are forming a phenotype which is called epithelial-mesenchymal transition (EMT) characterized by enhanced cell migratory features and reduced epithelial markers such as Cadherin 1, cytokeratin, and laminin.<sup>4,7,8</sup> *CDH1* itself is regulated by several microRNAs (miRNAs).<sup>9</sup> In general miRNAs play a major role in regulating EMT at the posttranscriptional level.<sup>4</sup> They regulate EMT through suppressing the expression of transcription factors in interaction with mediators like transcriptional repressors, histone methyltransferases, and ubiquitin-protein ligases.<sup>10</sup> The very complex participation of many miRNAs in the EMT scenario is described extensively in a study of Abba et al.<sup>11</sup> In conclusion it can be stated that the regulatory role of miRNAs in cell homeostasis is still a challenging research field where presumably many interactions and interactants have not been discovered yet.

MiRNAs are a growing family of short single-stranded noncoding RNA which are able to control gene expression by binding with their seed sequence to, that is, the 3' UTR region of messenger RNAs (mRNAs). Because these binding capabilities are not limited to one specific mRNA, the miRNAs are controlling multiple target genes at once.<sup>12–14</sup> Studies also show that miRNAs which are embedded in key genes are important regulators in many cellular pathways.<sup>15,16</sup> It seems that a majority of the genes are susceptible to be targeted by miRNAs. However, still a reasonably large number of 6000 miRNAs might be still undiscovered.<sup>17</sup> So far only approximately 2500 human miRNAs have been registered by the miR-Base consortium (<http://www.mirbase.org/>). The size of

mature miRNAs is ranging from 16 to 28 nucleotides in length with the most abundant form at 22 nucleotides having their binding region (seed sequence) at the 5' end with a size of 6–7 bases.<sup>18</sup>

The procedures to discover novel miRNAs were based for a long time on techniques like cloning and sequencing, but this approach has several limitations like the small size of miRNAs and their low abundance.<sup>19</sup> Therefore, the use of search tools to detect folded RNA motives (hairpins) followed by their experimental verification is an established approach to identify novel miRNAs. The existing tools for miRNA prediction consider different features of the miRNAs such as phylogenetic conservation, secondary structure information, and similarity to known miRNAs.<sup>20,21</sup>

Much is known about miRNAs that act on the human hub and tumor suppressor gene *CDH1*. But up to now, no miRNA is known which is coded by the open reading frame (ORF) of *CDH1* itself despite the intronic regions of *CDH1* are huge. Therefore, the present study is searching for the existence of miRNAs in the genomic sequence of *CDH1* to further define its important role in the EMT phenotype and to characterize putative candidates. The study is divided in a theoretical part searching for miRNA candidates and gene binding sites and a practical part based on several assays to validate the expression and discover the putative role of the candidate miRNAs.

## 2 | MATERIAL AND METHODS

### 2.1 | MiRNA hairpin structure prediction

The ORF of *CDH1* is approximately 100 kbp in length and consists of 16 exons and 15 introns. Up to now, no miRNA has been mapped in the *CDH1* locus. MiRNAfold online classifier<sup>22,23</sup> (<https://evryrna.ibisc.univ-evry.fr/miRNAfold>), MIREval<sup>24</sup> (<http://mimirna.centenary.org.au/mireval>), and SSC profiler<sup>25</sup> (<http://mirna.imbb.forth.gr/SSCprofiler.html>) programs were used to search for stable stem-loop structures within the encoding sequence of *CDH1*. For the first two tools, fasta files of the GRCh38

build of the human genome were used while in the third approach hg17 physical positions of the region of interest were provided. In all cases, the software defaults were applied. The UCSC genome database<sup>26</sup> (<http://genome.ucsc.edu/>) was utilized to analyze the conservation status of the putative miRNA sequences and their precursor sequence. A high score of conservation between similar species is seen as supportive for the existence of presumably active miRNA sequences.<sup>27</sup>

The bioinformatics tools microRNA-dis<sup>28</sup> (<http://bioinformatics.hitsz.edu.cn/microRNA-dis/server>), i-PseDPC<sup>29</sup> (<http://bioinformatics.hitsz.edu.cn/iMiRNA-PseDPC/>), and iMiRNA-SSF<sup>30</sup> (<http://bioinformatics.hitsz.edu.cn/iMiRNA-SSF/index.jsp>) tools were used for the determination of the mature miRNAs directly from their hairpin structures or to determine if the hairpin structure conforms to a valid pre-miRNA structure. Other in silico tools which were tested turned out to be less stringent like MiRmat<sup>31</sup> (<https://mcube.nju.edu.cn/jwang/lab/soft/MiRmat>), MatureBayes<sup>32</sup> (<http://mirna.imbb.forth.gr/MatureBayes.html>), and miRdup<sup>33</sup> (<http://wheat.bioinfo.uqam.ca./index.php?action=mirdup>) and were not considered.

Similarity analysis to existing miRNAs (miRBase version 22, human) was done by FASTA<sup>34</sup> ([https://fasta.bioch.virginia.edu/fasta\\_www2/fasta\\_www.cgi](https://fasta.bioch.virginia.edu/fasta_www2/fasta_www.cgi)) and BLASTN<sup>35</sup> (download version blast+ v.2.12.0) using their default values.

## 2.2 | Pathway analysis

To find potential target genes for the novel miRNA, initially the DIANA microT tool<sup>36</sup> (<http://diana.imis.athena-innovation.gr/DianaTools>) was used but finally we decided to go for miRDB<sup>37</sup> (<http://mirdb.org/>) for a focused search for the more important targets in the 3' UTR regions. The ranked result sets were analyzed for known oncogenes and enriched GO terms by R (v.4.1) with the primary libraries DOSE, clusterProfiler, and pathview. The resulting target genes were further analyzed if they are part of known protein complexes by a CORUM database search<sup>38</sup> (<https://mips.helmholtz-muenchen.de/corum/>) implemented in R. This method helps to define the biological role of the target genes. The R code is available on request.

## 2.3 | Cell lines and culture conditions

HEK293T, MCF7, MDA-MB-231, SW480, and HT-29 cell lines were cultured in DMEM-HG media (Gibco, Thermo

Fisher Scientific). HUVEC cell line was cultured in DMEM-F12 (Gibco, Thermo Fisher Scientific) and A549 cell line was cultured in RPMI-1640 media (Gibco, Thermo Fisher Scientific). All three media were supplemented with 100 U/ml penicillin, 100 µg/ml streptomycin (Sigma, Merck), and with 10% heat-inactivated fetal bovine serum (Invitrogen, Thermo Fisher Scientific). The cells were incubated in a standard way by 37°C, humid condition, and 5% CO<sub>2</sub>. All cell lines were obtained from Pasteur Institute, Tehran, Iran. HUVEC cells are derived from human umbilical vein endothelial cells and HEK293T is a sub-cell line derived from HEK293 original cell line that is transfected with a plasmid vector holding the SV40 origin of replication. The first cell line can be termed normal while the second cell line is slightly altered but still often used as a quasi-normal reference. MCF-7 which represents the most common form of breast cancer is positive regarding ER, PR, and negative in Her2, while MDA-MB-231 is a triple-negative cell line, therefore representing different cancer subgroups. Both cell types are derived from the epithelial layer of the mammary gland. SW480 and HT-29 are originated from intestinal epithelial layer, diagnosed as adenocarcinoma. A549 is derived from epithelial cells of the lung and is diagnosed as carcinoma. Further properties of the breast cancer cell lines can be seen in Dai et al.<sup>39</sup>

## 2.4 | Recombinant plasmid construction

The standard procedures are all based on protocols provided in the book "Molecular Cloning: A Laboratory Manual."<sup>40</sup> The flanking genomic region of 394 bp containing the putative hairpin structure was amplified using two primers called F-pre-CDH1-i2-miR1 and R-pre-CDH1-i2-miR1 (Table 1). The obtained polymerase chain reaction (PCR) product was cloned into the linear pTG19-T vector, subjected to enzymatic digestion using EcoRI and HindIII enzymes, and finally subcloned into the pEGFP-C1 expression vector downstream of the GFP gene. The miRNA precursor for the exogenous expression experiments was chosen based on quadruplex PCR using F-C1 forward and R-C1 reverse primers (Table 1). The vector construct was brought into cells to assure that the cells are able to process the mature miRNA out of the precursor form.

## 2.5 | Transfection of the HEK293T cells

Recombinant pEGFP-C1 expression vector containing *CDH1-i2-miR-1* precursor was transfected into HEK293T

TABLE 1 The list of used primers ordered by first occurrence

Primer name	Primer sequence, 5'–3'	Purpose
F-M13	GTAAAACGACGGCCAGT	Forward primer on backbone of TA cloning vector
R-M13	CAGGAAACAGCTATGAC	Reverse primer on backbone of TA cloning vector
F-C1	AGTCCGCCCTGAGCAAAG	Forward primer on backbone of pEGFP-C1 vector
R-C1	ACAAATGTGGTATGGCTGATTATG	Reverse primer on backbone of pEGFP-C1 vector
F-pre CDH1-i2-miR-1	TTCAGCAAATGCTCTTGAAG	Forward primer to amplify precursor structure
R-pre CDH1-i2-miR-1	ATTCCACAACGGCTTTCCTGT	Reverse primer to amplify precursor structure
F2-CDH1-i2-miR-1	GACTGTGGGAAATGCCTC	Final primer for identification of the miRNA
R-outer	GTCACTCTGCTCACTGG	Reverse primer on the anchor
R-inner	GCTTGAGCTCGAGTCCTC	Ditto.
F-SNORD48 (U48)	TGACCCAGGTAACCTCTGAGTGTGT	Internal control for miRNA expression in cell lines
F-GAPDH	GCCACATCGCTCAGACAC	Internal control for gene expression in cell lines
R-GAPDH	GGCAACAATATCCACTTTACCAG	Ditto. reverse primer
R-Anchored Oligo dT	GCGTCGACTAGTACAACCTCAAGGTTCTTC CAGTCACGACGT <sub>18</sub> X	Anchored oligo dt primer for cDNA synthesis in miRNA amplification. X: is G for cell line experiments and GAA for tissue samples.
F-miR-191-5p	CGGAATCCCAAAGCAG	Internal control for miRNA expression analysis in tissue samples
F-5S rRNA	ATCTCGGAAGCTAAGCAGGGTCCG	2 cd internal control
F-miR-21-5p	GGCGTAGCTTATCAGACTGATG	Forward primer to detect hsa-miR-21-5p in breast tissue samples
F-BAX	CCCGAGAGGTCTTTTTCCGAG	Forward primer to detect BAX expression after overexpression of CDH1-i2-miR-1
R-BAX	CCAGCCCATGATGGTTCTGAT	Ditto. reverse primer
F-PTEN	AGGGACGAACTGGTGAATGA	Forward primer to detect PTEN expression after overexpression of CDH1-i2-miR-1
R-PTEN	CTGGTCCTTACTTCCCCATAGAA	Ditto. reverse primer
F-CDH1	AGTGCCAACTGGACCAT	Forward primer to detect CDH1 expression after overexpression of CDH1-i2-miR-1
R-CDH1	CGGCCCTTCACAGTCACA	Ditto. reverse primer

Abbreviations: miRNA, microRNA; rRNA, ribosomal RNA.

cells using TurboFect transfection reagent (Thermo Scientific). About  $2 \times 10^5$  cells were seeded in 12-well plates, incubated 24 h. After that 2  $\mu$ g of recombinant pEGFP-C1 expression vector were diluted in 200  $\mu$ l serum-free DMEM and 3.5  $\mu$ l of TurboFect transfection reagent was added. This mixture was given to each well and 24, 48, and 72 h posttransfection amount and accuracy of the transfection was checked with a fluorescence microscope (Nikon eclipse Te2000-s). The maximum amount of transfection was observed by 48 h and was chosen for the exogenous verification. The pEGFP-C1 empty vector was used as a control for the transfection assay. Transfected and nontransfected cells were cultured identically.

## 2.6 | Quantitative PCR (qPCR) verification of the mature miRNA

Total RNA was extracted from transfected cells at 48 h using Trizol (Invitrogen) according to the manufacturer's protocol. A poly-A tail was added to 1  $\mu$ g of extracted RNA using poly-A polymerase enzyme (NEB). One hundred nanograms were taken for complementary DNA (cDNA) synthesis using the R-Anchored OligodT primer (Table 1). qPCR (StepOne, Applied Biosystems) was performed using one specific primer based on the predicted mature form of miRNA (F2-CDH1-i2-miR-1, Table 1) and a universal reverse primer. PCR conditions

are as follows: 95°C denaturation step for 15 s, 58°C annealing for 20 s, 72°C polymerization for 20 s, running 40 cycles. Amplification was performed using the Ampliqon RealQ Plus 2x Master Mix Green (Ampliqon) and each experiment was done in duplicates. qPCR data were normalized by U48 small nucleolar RNA (SNORD48) as the internal control and analyzed using the  $2^{-\Delta\Delta C_t}$  ratio.<sup>41</sup>

## 2.7 | Analyzing cell proliferation using the 3-(4,5-dimethylthiazol-2-yl)-2,5-diphenyltetrazolium bromide (MTT) assay

An MTT assay provides a quantitative measure of the cell viability. Cells were seeded in a 96-well plate at  $10^4$  cells/well, cultured until they reach a 60% confluence, and transfected with a recombinant vector system.<sup>42</sup> 24, 48, and 72 h posttransfection, MTT was added (final concentration 5 mg/ml) to each well and plates were incubated at 37°C for 4 h. After careful removal of the MTT solution, 150  $\mu$ l of dimethyl sulfoxide was added and plates were incubated at 37°C for 10 min. Finally, the absorbance was measured at 570 nm by a microplate reader (Biotek ELx800).

## 2.8 | Flow cytometry and fluorescence-activated cell sorting (FACS) procedures

Transfected and nontransfected HEK293T cell lines were harvested 48 h posttransfection for cell cycle analyses. The cells were suspended in propidium iodide (PI, Thermo Fisher Scientific) and annexin V/7-AAD (BioLegend) according to the manufacturer's protocol. All assays were performed in duplicates. Analysis of samples was done with a BD FACSCalibur flow cytometer with Cell Quest software (BD Biosciences) and analyzed by Flowing software v.2.5.1 (BD Biosciences, <https://bioscience.fi/services/cell-imaging/flowing-software/>).

## 2.9 | Endogenous CDH1-i2-miR-1 verification by quantitative real-time-PCR (qRT-PCR)

Two normal (HEK293T and HUVEK) and five cancerous cell lines (breast cancer: MCF7, MDA-MB-231, colon cancer: SW480, HT-29, and lung cancer: A549) were used. Total RNA was extracted from these cells and subjected to qPCR to determine endogenous expression of the identified miRNA in the different cell lines. The differences of the normal versus cancer situations were analyzed.

The 35 breast cancer tissues and its marginal normal tissues were attained from Kerman Nime-Shaban Clinic. Each sample was examined by two pathologists (Table 2). All tissue samples were immediately frozen in liquid nitrogen after departing from surgery and then stored at  $-80^\circ\text{C}$  until RNA isolation. The women of the study have an average age of 50.7 years (range 34–81). The patient samples were categorized based on the tumour, node and metastasis staging system (TNM) and grading system. All except one case belongs to the ductal breast carcinoma type. The grade included 9 samples of Grade I, II and 26 samples of Grade II/III and III. The stage groups included 19 samples in Stage II (II, IIA) and 9 samples in Stage III (IIIA, IIIB, IIIC). All the clinical data of the patients are provided in Table 2.

Total RNA was extracted from the tissue samples by using DENA RNA extraction solution according to the manufacturer's protocol (DENAzist Asia). RNA was analyzed for purity through density spectrophotometry and gel electrophoresis. For miRNA detection, a poly-A tail was added to 3' end of RNA using poly-A polymerase enzyme (NEB) followed by cDNA synthesis by reverse transcriptase enzyme (Fermentas). qRT-PCR was done by Ampliqon SYBR green Master Mix in the Applied Biosystems StepOne Real-Time PCR. hsa-miR-191-5p and 5S ribosomal RNA (rRNA) were used as internal controls. The relative expression level was calculated by the  $2^{-\Delta\Delta C_t}$  ratio.<sup>41</sup>

## 2.10 | Statistical analysis

All calculations were done in R (v.4.1) or GraphPad Prism 5.04 (GraphPad). Significant group differences were evaluated by *t* test and in case by variance adjusted procedures (Welch's *t*-test). In the case of qPCR differentiation analysis on breast cancer samples, paired *t*-test was applied. Multiple testing correction (Benjamini–Hochberg) was applied where necessary. The significance level was set in all cases to 5%. The significance levels in figures were denoted by stars representing *p*-value ranges: n.s.: not significant, \**p* < 0.05, \*\**p* < 0.01, \*\*\**p* < 0.001, \*\*\*\**p* < 0.0001.

## 3 | RESULTS

### 3.1 | Computational prediction of putative miRNA sequences in the CDH1 gene

The application of MiRNAfold, MIREval, and SSCprofiler revealed several stable hairpin structures across the

Patient number	Grade	Staging	Type	Age	Sex
1	II	T2 NX MX (II)	Ductal	34	Female
2	II/III	T4 N1 MX (IIIB)	Ductal	81	Female
3	II	T2 N3 MX (III)	Ductal	50	Female
4	III	T2 N3 MX (IIIC)	Ductal	73	Female
5	II	T2 N0 MX (IIA)	Ductal	41	Female
6	II	T2 N0 MX (IIA)	Ductal	36	Female
7	II/III	T2 Nx MX (IIA)	Ductal	35	Female
8	II/III	T2 N0 MX (IIA)	Lobular	68	Female
9	II/III	T2 N0 MX (IIA)	Ductal	48	Female
10	II/III	T2 N0 MX (IIA)	Ductal	57	Female
11	II/III	T2 N0 MX (IIA)	Ductal	75	Female
12	II/III	T2 N0 MX (IIA)	Ductal	55	Female
13	II/III	T2 N1 MX (IIB)	Ductal	45	Female
14	II/III	T2 NX MX (IIA)	Ductal	66	Female
15	I	T2 N0 MX (IIA)	Ductal	46	Female
16	II/III	T2 N0 MX (IIA)	Ductal	48	Female
17	II/III	T2 N2 MX (IIIA)	Ductal	47	Female
28	II/III	T1 N1 MX (IIA)	Ductal	59	Female
19	II/III	T2 N2 MX (IIIA)	Ductal	48	Female
20	II	T1 N0 MX (II)	Ductal	45	Female
21	II/III	T2 N2 MX (IIIA)	Ductal	39	Female
22	III	T2 N0 MX (IIA)	Ductal	52	Female
23	I	T2 N0 MX (IIA)	Ductal	36	Female
24	II/III	T4 N0 MX (IIIB)	Ductal	53	Female
25	II/III	T2 N3 MX (IIIc)	Ductal	45	Female
26	II	T2 N0 MX (IIA)	Ductal	40	Female
27	II/III	T4 N3 MX (IIIC)	Ductal	39	Female
28	III	T2 N0 MX (IIA)	Ductal	41	Female
29	III	T2 N0 MX (IIA)	Ductal/medullary	65	Female
30	II/III	T2 NX MX (IIA)	Ductal	79	Female
31	II	T2 N0 MX (IIA)	Ductal	57	Female
32	III	T2 N0 MX (IIA)	Ductal	46	Female
33	II/III	T2 NX MX (IIA)	Ductal	35	Female
34	II/III	T2 N0 MX (IIA)	Ductal	43	Female
35	II/III	T2 N2 MX (IIIA)	Ductal	34	Female

TABLE 2 Clinical data of patient samples

*CDH1* ORF containing 16 exons. The minimum free energy values as indicators for stability were in the range of  $-23$  to  $-29$  kcal/mol. The in silico validation by iMiRNA-PseDPC, iMiRNA-SSF, and miRNA-dis give support that the selected precursor structures are valid

miRNA structures. From the 27 miRNA candidates, one well conserved and promising precursor sequence was selected which is located in the huge second intron of *CDH1* gene comprising approximately 64% of the ORF of the canonical transcript of *CDH1*. The predicted novel

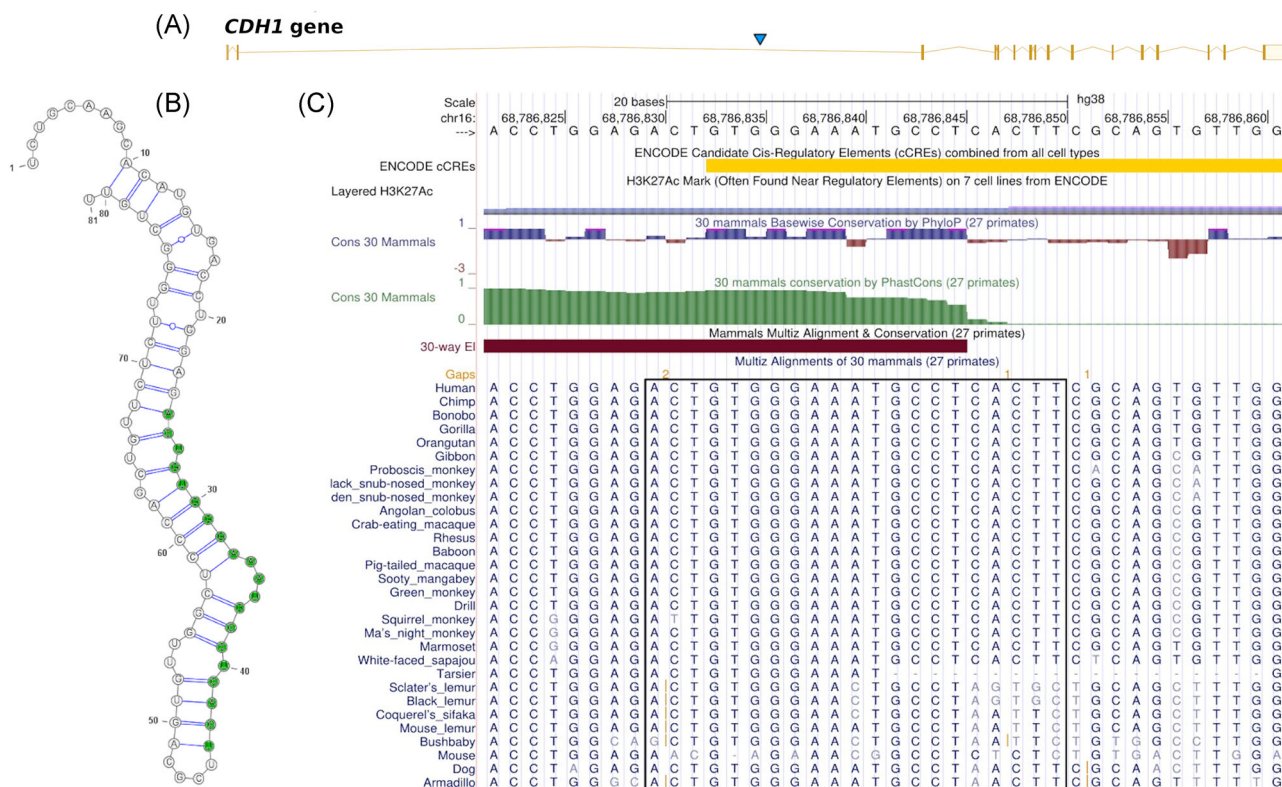


**FIGURE 1** Novel microRNA (miRNA) CDH1-i2-miR-1 and conservation status of the sequence. (A) The genomic structure of the canonical *CDH1* transcript contains 16 exons. The huge second intronic region between exon 2 and 3 is harboring the novel miRNA (blue triangle). It is quite obvious that intron two is having a lot of space for regulatory elements. (B) The candidate which passed all verification experiments is shown here folded to a secondary structure by MIREval. The genomic sequence is not including the possible U-to-C editing here. The secondary structure is symbolized by nucleotides in circles (green/white), partly paired (blue linker lines), and the location of the validated mature form is indicated by green circles. The computed minimum free energy is  $-23.2$  kcal/mol. (C) The UCSC database of the human genome (GRCh38/hg38) was used to show the conservation status of the sequence. Twenty-seven primates and three further mammals were included. The black box indicates the mature CDH1-i2-miR-1 sequence. It can be seen that the conservation status is high. On top, the sequence positions of chromosome 16 are given. The green and brown and bluish area graphs denote the conservation status by further algorithms as described inside the graph. In yellow, the ENCODE information on putative regulatory elements is given

miRNA was named provisionally CDH1-i2-miR-1 and its physical position is indicated in Figure 1A by a blue triangle. The hairpin structure of CDH1-i2-miR-1 calculated by MIREval is shown in Figure 1B.

A BLASTN and FASTA search of the detected CDH1-i2-miR-1 mature sequence (cf. 3.2) against all human mature sequences of the miRBase database showed that no registered miRNA sequence is identical to ours. Nevertheless, there are some sequence similarities with a continuous stretch of maximal nine nucleotides which is in line with values which can be observed for well-established miRNAs like hsa-miR-21-3p and hsa-miR-200a/b/c-3p as a reference (Supporting Information S1). Sometimes there is also some overlap in the seed sequence, but this observation can also be made using the same procedures for the reference miRNAs.

The BLASTN search (EBI-Ensemble) with the mature form of CDH1-i2-miR-1 against the human genome

revealed as expected the *CDH1* gene and two further very similar motives at chr19:4386842-4386858 (SH3GL1, reverse strand) and chr11:127371420-127371436 (no gene, reverse strand, Supporting Information S2).

The sequence of *CDH1-i2-miR-1* (cf. 3.2), is well conserved through several species (Figure 1C) based on the UCSC genome database and the GRCh38/hg38 release.

The analysis of putative gene targets for the 3'UTR region revealed based on a sliding window approach from physical start position chr16:68786827 to 68786839 several weaker to stronger overlapping gene sets (Figure S1). A remarkably higher than average overlap is at start position 68786831/2 and 68786833/4. In that range, the GO analysis also exposed 25–28 cancer genes in the standardized KEGG pathway sheet Hsa05200 (Figure S2). All the mentioned cancer genes show a miRDB rank score above the median.



### 3.3 | Cell viability is suppressed by CDH1-i2-miR-1

The HEK293T cells were transfected with a p-EGFP-C1 vector containing *CDH1-i2-miR-1* precursor sequences. The cells were harvested for the MTT assay at 24, 48, and 72 h posttransfection to assess the effects of mature *CDH1-i2-miR-1* on cell viability. The time point of 24 h was discarded because the transfection efficiency was too low. At 48 or 72 h posttransfection *CDH1-i2-miR-1* could decrease the number of viable cells significantly (Figure 3A). The maximal efficiency was at 48 h posttransfection. Therefore, this time was considered for subsequent experiments.

### 3.4 | CDH1-i2-miR-1 is endogenously expressed in tumor and normal cells at different rates

The *in vivo* activity of *CDH1-i2-miR-1* was evaluated using qPCR in two different normal cells HUVEC and HEK293T, and five cancerous cells MCF7, HT-29, MDA-MB-231, SW480, and A549. The expression of *CDH1-i2-miR-1* was significantly upregulated in HT-

29, and significantly downregulated in MDA-MB-231 and SW480 compared to the normal cell lines HUVEC and HEK293T (Figure 5A). MCF7 and A549 do not clearly differ from the controls. This broad expression range might point to different roles of this new miRNA in different pathophysiological states.

### 3.5 | CDH1-i2-miR-1 is inducing cellular apoptosis

The tumor suppressor effect of *CDH1-i2-miR-1* on cell cycle and apoptosis was analyzed by an annexin-7AAD assay. HEK293T cells were again transfected with an empty pEGFP-C1 vector and with a pEGFP-C1 expression vector containing the *CDH1-i2-miR-1* precursor. Figure 3B shows the percentage of cells in necrotic state, early- and late apoptosis, and pro-survival state. *CDH1-i2-miR-1* induction in cells increased the cell numbers in the early apoptosis stage from 20% to 33% compared to the control while the late apoptosis stage is only slightly increased from 2% to 5%. The percentage of living cells decreased after treatment compared to the control, confirming the initiation of apoptosis in these cells.

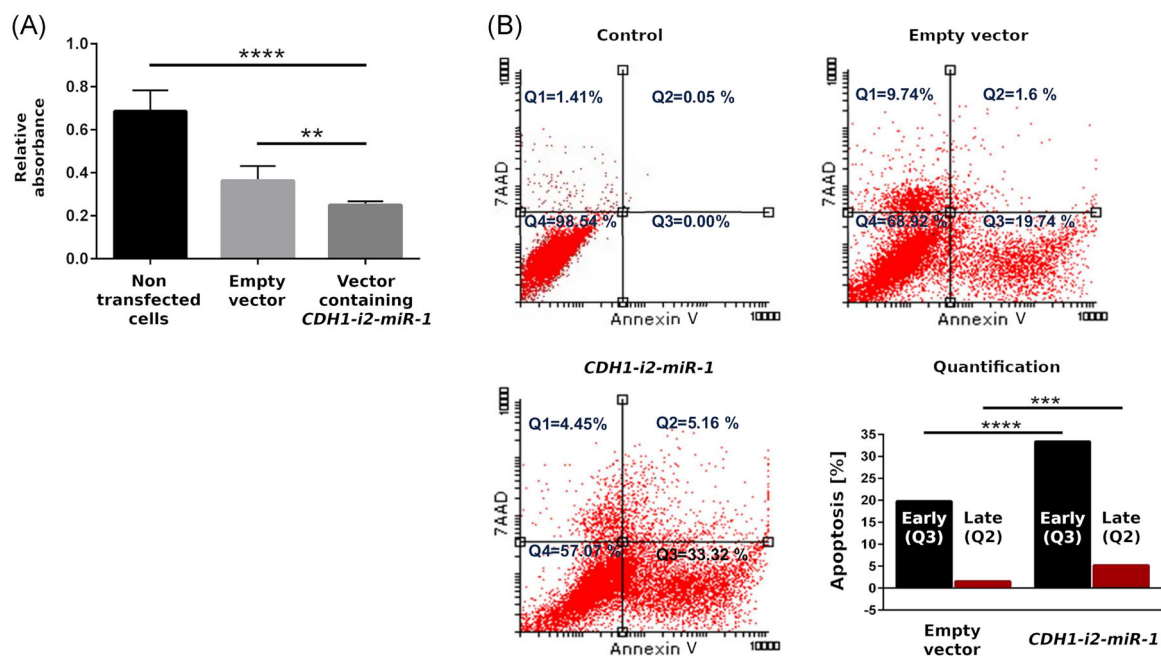


**FIGURE 3** *CDH1-i2-miR-1* affects the cell cycle and apoptosis in HEK293T cells. (A) The 3-(4,5-dimethylthiazol-2-yl)-2,5-diphenyltetrazolium bromide assay of *CDH1-i2-miR-1* after overexpression in HEK293T cells using two different incubation times of 48 and 72 h. The averaged results of both time points show that there is a significant decrease in cell viability in transfected cells compared to control cells. In the right panel (B), the flow cytometry results of *CDH1-i2-miR-1* on HEK293T cells using annexin-7AAD reveal more details. Control denotes cells without vector. Next, cells are transfected with an empty vector. Below, cells transfected with a vector containing the miRNA *CDH1-i2-miR-1* and to the right the quantification: black bars represent the early apoptosis area (Q3) while the dark-red bars denote the late apoptosis area (Q2). The results indicate that the percentage of transfected cells in early and late apoptosis is significantly increased by transfecting cells with *CDH1-i2-miR-1*

### 3.6 | CDH1-i2-miR-1 affects cell cycle

To test whether the apoptotic effect induced by CDH1-i2-miR-1 is associated with cell cycle arrest, HEK293T cells were treated with a recombinant pEGFP-C1 vector loaded with CDH1-i2-miR-1, stained by PI, and analyzed by FACS. As shown in Figure 4, significant changes were observed in the cell stages after treatment with CDH1-i2-miR-1. The percentage of cells in the G2/M phase after treatment with CDH1-i2-miR-1 increased from 19% in the control situation to 34%, while the percentage of cells in the G1 and S phases decreased. These results indicated that CDH1-i2-miR-1 inhibited cell proliferation very effectively by inducing cell cycle arrest at G2/M phase.

### 3.7 | CDH1-i2-miR-1 is differentially expressed in normal and breast tumor tissue samples

The differential expression of CDH1-i2-miR-1 was evaluated in 35 breast tumor specimens compared to their noncancerous marginal tissues (Figure 5B–D). The rationale for breast cancer resulted from the theoretical analysis at the beginning of the study and their pointers

to breast cancer but also because of its high incidence in Iran.<sup>47</sup> As a positive control hsa-miR-21-3p was measured in parallel. Two different internal controls hsa-miR-191-5p and 5S rRNA were tested for this experimental approach. hsa-miR-191-5p was finally chosen because of its low variation in breast samples. The observed good performance of hsa-miR-191-5p is consistent with results we published in a previous miRNA expression study.<sup>48</sup> In the primarily ductal invasive breast cancer cohort, CDH1-i2-miR-1 was downregulated (fc -3.95) and hsa-miR-21-3p upregulated (fc 2.42) both in relation to the paired normal tissue.

We also compared the expression of these two miRNAs in a subgrouping of patients with lower grades (Grade I + II) versus the higher grade (II/III + III). The expression of CDH1-i2-miR-1 was significantly more downregulated in higher grades. A trend but no significance could be established for a decreased in higher grades for hsa-miR-21-5p. This might suggest CDH1-i2-miR-1 as a progression marker in breast cancer and indicates a role in breast cancer progression.

Summing up all the results we could verify the presence and action of a new miRNA, provisionally termed CDH1-i2-miR-1, in the large second intron of *CDH1* and exemplified its in vivo occurrence in breast cancer

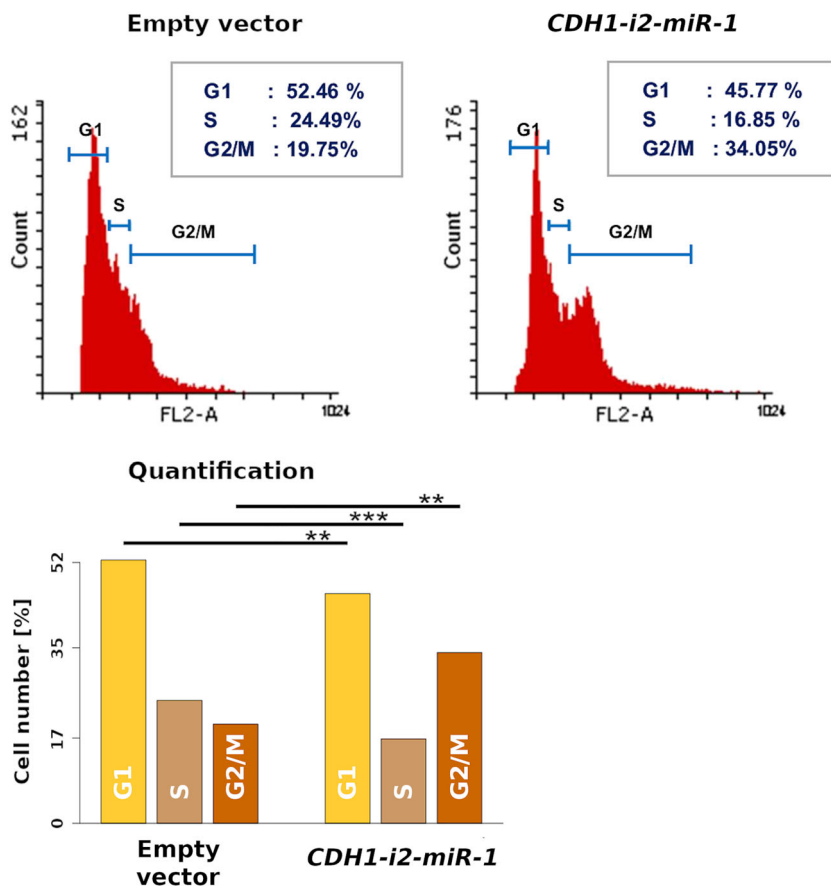


**FIGURE 4** CDH1-i2-miR-1 shows cell cycle arrest. In the bottom line, the flow cytometry results of HEK293T cells using propidium iodide staining expose a G2/M arrest. On the left, the cells are transfected with the empty vector. In the middle, cells were transfected with the vector containing *CDH1-i2-miR-1*. On the right, the cell count values (percent) from the G1 phase (yellow bar), S phase (brown bar), and G2/M phase (dark orange bar) of the two conditions. The statistical analysis supports the validity and stability of the differences between the three cell cycle phases

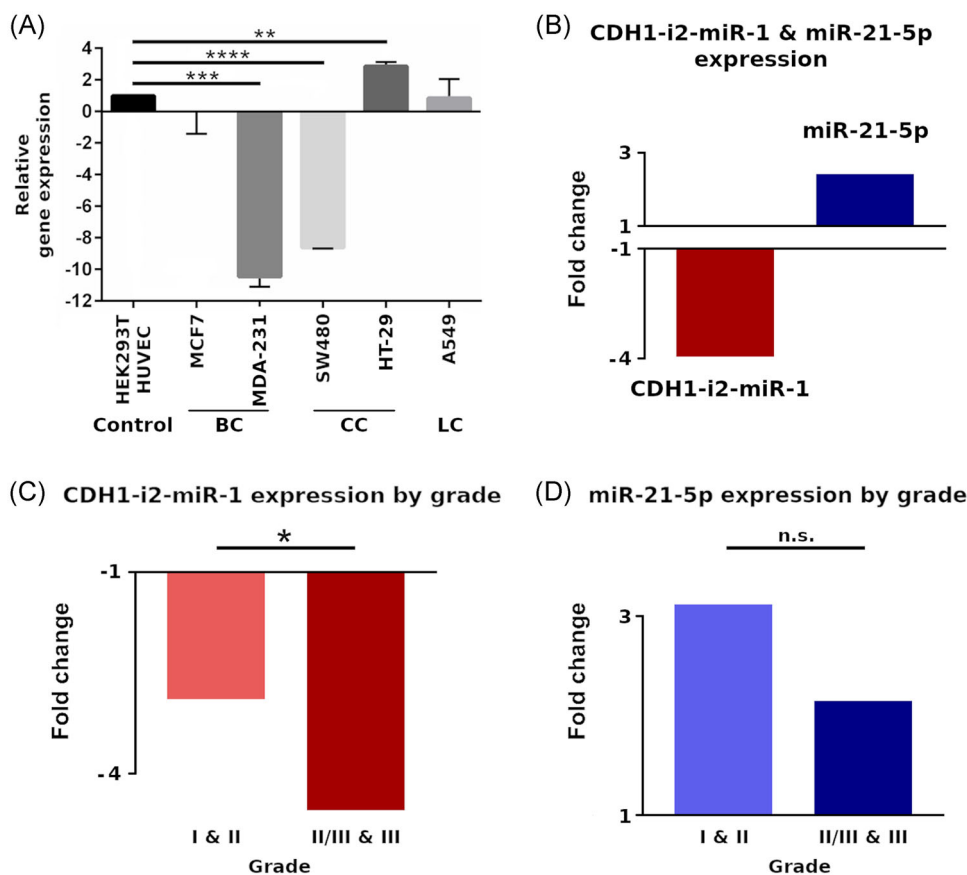


**FIGURE 5** CDH1-i2-miR-1 expression is bound to differentiation and physiological state. CDH1-i2-miR-1 expression in cell lines and tumor tissues of breast cancer samples. (A) The endogenous CDH1-i2-miR-1 expression is remarkably different across several tumor cell lines (BC, breast cancer; CC, colon cancer; LC, lung cancer). The expression of the tumor cell lines is shown in relation to the average expression of both as normal defined cell lines HUVEC and HEK293T. (B) The panel shows the antagonistic activity of the microRNA (miRNA) CDH1-i2-miR-1 (fc  $-3.95$ , decreased) and as a positive control hsa-miR-21-5p (fc  $2.42$ , increased). The measurement is based on the internal control hsa-miR-191-5p. The left bar (black) denotes adjacent normal breast tissue as a reference. (C and D) The expression pattern of each miRNA was assessed based on their grading. The expression of CDH1-i2-miR-1 is significantly more downregulated in Grade II/III and III compared to Grade I and II. A trend but no significant difference (n.s.) was observed concerning the positive control of miRNA hsa-miR-21-5p

samples. The expression of CDH1-i2-miR-1 in comparison to the well-characterized miRNA hsa-miR-21-5p and based on the internal control hsa-miR-191-5p shows a comparable strength but acts in an antagonistic way. The new miRNA CDH1-i2-miR-1 might take part in cell cycle regulation and apoptosis.

## 4 | DISCUSSION

Due to the importance of Cadherin 1 in EMT and its involvement in oncogenesis, we searched for the presence of regulatory miRNAs in its ORF by bioinformatics procedures. The selected candidate miRNA provisionally termed CDH1-i2-miR-1 was verified by cloning and exogenous validation studies. An extensive pathway analysis to reveal the biological role of the new miRNA

was performed and lead to several cancer-related pathways. The lab assays indicate possible functions of the new miRNA in breast cancer pathogenesis and exemplified the role of CDH1-i2-miR-1 in the regulation of the cell cycle and apoptosis.

The detection of miRNAs is complicated by their small size and their often low abundance in tissue samples and cell cultures. So, the combination of bioinformatical approaches with experimental verification studies is a helpful strategy to identify and annotate a novel miRNA. Because of bioinformatic tools differ often by their theoretical concepts and their algorithmic implementations and therefore have their own specificity, we used three tools in parallel to generate stable miRNA candidates.<sup>49</sup> The resulting stable and conserved miRNA candidate is located in the second intron of *CDH1* and therefore can be termed intronic miRNA which is the

greatest group of miRNAs.<sup>50</sup> The analysis of different *CDH1-i2-miR-1* lengths on the 5' end resulting in different seed regions revealed different gene target sets. The adjacent target sets overlap in a certain way but some overlaps are remarkably higher. This might indicate the natural seed sequence which in our case is associated prominently with cancer pathways. The GO analysis of predicted target genes as well as the appearance of the corresponding proteins in protein complexes expose several interesting cancer-related pathways and processes. The performed experiments in turn support these theoretical observations. The sequence of *CDH1-i2-miR-1* is very unique and the sequence overlap to existing miRNAs is in line with well-characterized reference miRNAs. Two very homologous genomic regions exist. One on chromosome 19, *SH3GL1*, part and activator of the EGFR/ERK/NF-kappa B signaling and further cancer-associated pathways<sup>51,52</sup> might have a similar cancer characteristic compared to *CDH1*. The other on chromosome 11 is located in an intergenic region and no annotation is available. These miRNA regions are not described to our knowledge up to now.

The *CDH1-i2-miR* precursor structure is processed to a mature miRNA. The exogenous expression of the mature miRNA followed by Sanger sequencing revealed a sequence which might be posttranscriptionally edited in one 3' base. As already mentioned, the U-to-C editing might be a less common event but in-depth studies are still rare.<sup>43,44</sup>

The small functional experiment with *CDH1-i2-miR-1* overexpression on *BAX*, *PTEN*, and *CDH1* is additionally underlining the scope of *CDH1-i2-miR-1* action. No self-regulation but a clear effect on apoptosis and cell cycle via *BAX* and *PTEN*. *BAX* is reported to be a proapoptotic protein<sup>53</sup> which regulates programmed cell death by inducing mitochondrial permeability transition.<sup>54</sup> The last study also showed that overexpression of *BAX* in Jurkat cells is initiating programmed cell death within 2 h. They also observed typical manifestation of apoptosis by caspase activation, DNA fragmentation, and cytochrome C release following *BAX* overexpression. *PTEN* is described as a tumor suppressor which regulates cell growth, cell cycle, and apoptosis.<sup>55</sup> Li et al. showed that *PTEN* overexpression suppresses cell growth and induces apoptosis in human breast cancer cells by inhibition of the PI3K/AKT or MAP kinase pathways. Moreover, reexpression of *PTEN* in various tumor cell lines enhances apoptosis.<sup>56</sup>

*CDH1-i2-miR-1* is the first miRNA reported in the *CDH1* gene. This is curious for such a large gene. Therefore we were interested to see if for other members of this superfamily of Cadherins already miRNAs were reported. Rahimi et al.<sup>57</sup> showed the presence of a novel

miRNA in *CDH4*'s ORF likewise embedded in the similar sized second intron of the *CDH4* gene. This miRNA was also linked to cancer pathways and has a role in cell migration. Despite these parallels, the overall structure of *CDH1* and -4 is different and they are hosted on different chromosomes. Nevertheless, it seems that intronic miRNAs can be coded by Cadherins.

Several further regulatory elements are already reported in the second intron of *CDH1*. It has to be noted that in recent years, the physical position of the *CDH1* gene has slightly changed. Nevertheless, the positions of further and already described regulatory sequence motifs could be located and neither own a direct overlap to *CDH1-i2-miR-1* nor are in close vicinity. In particular, the comprehensive publication of Stemmler et al.<sup>58</sup> is describing one tissue-specific genomic enhancer region (tse3) on the upstream side of *CDH1-i2-miR-1*. But this region is not further characterized in this publication and therefore it could only be speculated that this region might rule *CDH1-i2-miR-1*. Pinheiro et al.<sup>59</sup> described four alternate transcripts which are characterized by a new starting exon inside intron 2–3 but the alternate exons do not overlap with the *CDH1-i2-miR-1* region which is more or less in the middle of the (alternate) intronic region 1–2 in these transcripts. Tedaldi et al.<sup>60</sup> tries to widen the epigenetic aspect for the regulatory elements of *CDH1* especially in gastric cancer. *CDH1-i2-miR-1* is situated between two FANTOM5 enhancers there termed F and G and at the flank of a small chromatin alteration peak of the histone H3 (H3K27Ac established from normal stomach cells). The methylation status of the two enhancers F and G shows that all eight analyzed gastric cancer cell lines have merely fully methylated CpG islands and there is no differential behavior between the cell lines. It does not seem that the reported structural features directly interact with the *CDH1-i2-miR-1* region or explain expression of *CDH1-i2-miR-1*.

Cell viability assay showed that *CDH1-i2-miR-1* overexpression decreases the number of live cells significantly. This led us to see if this overexpression influence apoptosis and cell cycle as well. Annexin V/7AAD staining showed both early and late apoptosis are affected by *CDH1-i2-miR-1* overexpression and the cells arrested significantly at the G2/M stage. These three observations expose *CDH1-i2-miR-1* involvement in cell cycle regulation and apoptosis and define its tumor suppressor characteristics. In accordance with these results, our GO analysis concerning cancer pathways resulted in *CDK4/6*<sup>61,62</sup> and *PI3K*<sup>63</sup> as two main players of cell growth. Additionally, two further molecular players for apoptosis, *APAF1* and cytochrome c (*CYCS*) showed up in the cancer pathway analysis.<sup>64</sup> These two molecules are important components of the apoptosome and

play a major role in initiating the programmed cell death.<sup>64–66</sup>

The significant alteration of CDH1-i2-miR-1 expression in breast (MDA-MB-231) and colorectal (SW480 and HT-29) cell lines compared to normal cell lines showed that CDH1-i2-miR-1 plays a relevant role not only in breast cancer. The exception of breast cancer cell line MFC7 and lung cancer cell line A549 indicates that even cancer subtypes might behave differently. Due to our interest in ductal invasive breast cancer, a growing disease in Iran, we evaluated the expression pattern of CDH1-i2-miR-1 in 35 breast cancer tissues and found it significantly downregulated in accordance with the established tumor suppressor phenotype of CDH1-i2-miR-1. In contrast, the expression of hsa-miR-21-5p which is a prominent oncogene was upregulated in these samples. This opposite expression of CDH1-i2-miR-1 compared to hsa-miR-21-5p is in line with the further experimental observations of cell cycle arrest under CDH1-i2-miR-1 induction and less cell viability in the MTT assay.

We also observed that CDH1-i2-miR-1 expression was significantly upregulated between cancer Grade I/II and III while stage classification was a less valid factor for distinction. Such a clear difference in the grade situation was not observed in the case of the positive control hsa-miR-21-5p. Qian et al.<sup>67</sup> could observe a grade but not stage dependency in hsa-miR-21-5p while Wang et al.<sup>68</sup> who assessed the plasma levels of hsa-miR-21-5p in benign and breast cancer samples shows an increase in expression with increased stage but did not analyze the grade. Nouraei et al. reported that hsa-miR-21-5p was infiltrating the marginal tissues and fibroblast cells there could elevate the hsa-miR-21-5p expression levels. This could partly explain why our expected differential values for our control miRNA hsa-miR-21-5p were insignificant.<sup>69</sup> Overall, the validity of the CDH1-i2-miR-1 grade dependency seems to have a strong evidence.

The putative action of CDH1-i2-miR-1 on cancer-related genes based on the pathway maps shown in Figure S2 are diverse. The common interaction candidates are growth factors (TGFBR1, FGFR1<sup>70,71</sup>), kinases (CDK4, MAPK8, PIK3CA<sup>72,73</sup>), a kinase inhibitor which is acting on CDK4/6 and is an effector of the TGFBR1 induced cell cycle arrest (CDKN2B<sup>74</sup>), a G protein (GNA11<sup>75</sup>), a cyclase ADCY1 which takes part in cAMP signaling<sup>76</sup> in response to G-protein signaling, a mediator of structural elements (CTNNA1<sup>77</sup>), and bone differentiation factor (BMP2<sup>78</sup>) inducing EMT and stemness of breast cancer cells via the Rb/CD44 pathways. The WNT pathway might also be involved by Frizzled (FZD7, eventually further family members), or Dvl.<sup>79</sup> All the factors show relevance in tumor processes, especially breast cancer, and together point,

that is, towards cell division, metastasizing, and dedifferentiation.

## 5 | CONCLUSION

The first novel miRNA CDH1-i2-miR-1 in the second intron of *CDH1* is opening perspectives to understand the activity of Cadherin 1 on other pathway proteins in a more consistent way. The activity of CDH1-i2-miR-1 is addressing the cell cycle and the apoptosis pathway and these interactions underline the important function of Cadherin 1 as a hub molecule in the EMT process. The effect of CDH1-i2-miR-1 overexpression on *BAX* and *PTEN* is consistent with a tumor suppressor role. The observations that CDH1-i2-miR-1 is differentiating tumor grade in breast cancer suggest it as a marker for tumor progression. The predicted cancer-related downstream targets show the potential of the CDH1-i2-miR-1 miRNA in the context of tumor biology.

## ACKNOWLEDGMENTS

This study was funded by Kerman Medical University, grant number 96000216. We also acknowledge support from the Open Access Publication Fund of the University of Münster.

## CONFLICT OF INTERESTS

The authors declare that there are no conflict of interests.

## ETHICS STATEMENT

The primary study was conducted according to the guidelines of the Declaration of Helsinki and approved by the Ethics Committee of Kerman Medical University Ethical Board (1396.1297). Informed consent was obtained from all subjects involved in the study.

## AUTHOR CONTRIBUTIONS

*Conceptualization:* Sedigheh Gharbi and Zahra Mohammadi. *Methodology:* Sedigheh Gharbi, Zahra Mohammadi, Maryam Saedi Dezaki, and Eberhard Korsching. *Software:* Sedigheh Gharbi, Zahra Mohammadi, and Maryam Saedi Dezaki. *Validation:* Sedigheh Gharbi, Zahra Mohammadi, and Maryam Saedi Dezaki. *Investigation:* Sedigheh Gharbi, Zahra Mohammadi, Maryam Saedi Dezaki, Sadat Dokanehiifard, Shahriar Dabiri, and Eberhard Korsching. *Resources:* Sadat Dokanehiifard and Shahriar Dabiri. *Writing-original draft preparation:* Sedigheh Gharbi, Zahra Mohammadi, Maryam Saedi Dezaki, Sadat Dokanehiifard, Shahriar Dabiri, and Eberhard Korsching. *Writing-review and editing:* Sedigheh Gharbi and Eberhard Korsching. *Supervision:* Sedigheh Gharbi and Eberhard Korsching. *Funding acquisition:* Sedigheh Gharbi and Eberhard Korsching. All authors

have read and agreed to the published version of the manuscript.

## DATA AVAILABILITY STATEMENT

The data are contained within the article or supplementary material.

## ORCID

Eberhard Korsching  <http://orcid.org/0000-0001-9141-1988>

## REFERENCES

- Oda H, Takeichi M. Evolution: structural and functional diversity of cadherin at the adherens junction. *J Cell Biol.* 2011; 193(7):1137-1146. doi:10.1083/jcb.201008173
- van Roy F. Beyond E-cadherin: roles of other cadherin superfamily members in cancer. *Nat Rev Cancer.* 2014;14(2): 121-134. doi:10.1038/nrc3647
- Mendonça AM, Na TY, Gumbiner BM. E-cadherin in contact inhibition and cancer. *Oncogene.* 2018;37(35):4769-4780. doi:10.1038/s41388-018-0304-2
- Wong SHM, Fang CM, Chuah LH, Leong CO, Ngai SC. E-cadherin: its dysregulation in carcinogenesis and clinical implications. *Crit Rev Oncol Hematol.* 2018;121:11-22. doi:10.1016/j.critrevonc.2017.11.010
- Kourtidis A, Lu R, Pence LJ, Anastasiadis PZ. A central role for cadherin signaling in cancer. *Exp Cell Res.* 2017;358(1): 78-85. doi:10.1016/j.yexcr.2017.04.006
- Navarro P, Gómez M, Pizarro A, Gamallo C, Quintanilla M, Cano A. A role for the E-cadherin cell-cell adhesion molecule during tumor progression of mouse epidermal carcinogenesis. *J Cell Biol.* 1991;115:517-533. doi:10.1083/jcb.115.2.517
- Gravdal K, Halvorsen OJ, Haukaas SA, Akslen LA. A switch from E-cadherin to N-cadherin expression indicates epithelial to mesenchymal transition and is of strong and independent importance for the progress of prostate cancer. *Clin Cancer Res.* 2007;13(23):7003-7011. doi:10.1158/1078-0432.ccr-07-1263
- Yao X, Ireland SK, Pham T, et al. TLE1 promotes EMT in A549 lung cancer cells through suppression of E-cadherin. *Biochem Biophys Res Commun.* 2014;455(3-4):277-284. doi:10.1016/j.bbrc.2014.11.007
- Rossi T, Tedaldi G, Petracchi E, et al. E-cadherin down-regulation and microRNAs in sporadic intestinal-type gastric cancer. *Int J Mol Sci.* 2019;20(18):4452. doi:10.3390/ijms20184452
- Mudduluru G, Abba M, Batliner J, et al. A systematic approach to defining the microRNA landscape in metastasis. *Cancer Res.* 2015;75:3010-3019. doi:10.1158/0008-5472.can-15-0997
- Abba M, Patil N, Leupold J, Allgayer H. MicroRNA regulation of epithelial to mesenchymal transition. *J Clinical Medicine.* 2016;5:8. doi:10.3390/jcm5010008
- Olejniczak M, Kotowska-Zimmer A, Krzyzosiak W. Stress-induced changes in miRNA biogenesis and functioning. *Cell Mol Life Sci.* 2018;75(2):177-191. doi:10.1007/s00018-017-2591-0
- Pradillo M, Santos JL. Genes involved in miRNA biogenesis affect meiosis and fertility. *Chromosome Res.* 2018;26(4): 233-241. doi:10.1007/s10577-018-9588-x
- Romero-Cordoba SL, Salido-Guadarrama I, Rodriguez-Dorantes M, Hidalgo-Miranda A. miRNA biogenesis: biological impact in the development of cancer. *Cancer Biol Ther.* 2014;15(11):1444-1455. doi:10.4161/15384047.2014.955442
- Cong, N, Du P, Zhang A, et al. Downregulated microRNA-200a promotes EMT and tumor growth through the wnt/beta-catenin pathway by targeting the E-cadherin repressors ZEB1/ZEB2 in gastric adenocarcinoma. *Oncol Rep.* 2013;29(4): 1579-1587. doi:10.3892/or.2013.2267
- Wong TS, Gao W, Chan JY. Interactions between E-cadherin and microRNA deregulation in head and neck cancers: the potential interplay. *BioMed Res Int.* 2014;2014:126038. doi:10.1155/2014/126038
- Alles J, Fehlmann T, Fischer U, et al. An estimate of the total number of true human miRNAs. *Nucleic Acids Res.* 2019;47: 3353-3364. doi:10.1093/nar/gkz097
- Xu W, Lucas AS, Wang Z, Liu Y. Identifying microRNA targets in different gene regions. *BMC Bioinformatics.* 2014; 15(suppl 7):S4. doi:10.1186/1471-2105-15-s7-s4
- Berezikov E, Cuppen E, Plasterk RH. Approaches to microRNA discovery. *Nat Genet.* 2006;38(suppl):S2-S7. doi:10.1038/ng1794
- Saleh AJ, Soltani BM, Dokanehiifard S, Medlej A, Tavalaei M, Mowla SJ. Experimental verification of a predicted novel microRNA located in human PIK3CA gene with a potential oncogenic function in colorectal cancer. *Tumour Biol.* 2016; 37(10):14089-14101. doi:10.1007/s13277-016-5264-y
- Berezikov E, Guryev V, van de Belt J, Wienholds E, Plasterk RH, Cuppen E. Phylogenetic shadowing and computational identification of human microRNA genes. *Cell.* 2005;120(1):21-24. doi:10.1016/j.cell.2004.12.031
- Tav C, Tempel S, Poligny L, Tahi F. miRNAfold: a web server for fast miRNA precursor prediction in genomes. *Nucleic Acids Res.* 2016;44:W181-W184. doi:10.1093/nar/gkw459
- Tempel S, Tahi F. A fast ab-initio method for predicting miRNA precursors in genomes. *Nucleic Acids Res.* 2012;40:e80. doi:10.1093/nar/gks146
- Gao D, Middleton R, Rasko JEJ, Ritchie W. miREval 2.0: a web tool for simple microRNA prediction in genome sequences. *Bioinformatics (Oxford, England).* 2013;29:3225-3226. doi:10.1093/bioinformatics/btt545
- Oulas A, Boutla A, Gkirtzou K, Reczko M, Kalantidis K, Poirazi P. Prediction of novel microRNA genes in cancer-associated genomic regions—a combined computational and experimental approach. *Nucleic Acids Res.* 2009;37:3276-3287. doi:10.1093/nar/gkp120
- Kent WJ, Sugnet CW, Furey TS, et al. The human genome browser at UCSC. *Genome Res.* 2002;12:996-1006. doi:10.1101/gr.229102
- Yang, J-S, Phillips MD, Betel D, et al. Widespread regulatory activity of vertebrate microRNA\* species. *RNA (New York, N.Y.).* 2011;17:312-326. doi:10.1261/rna.2537911
- Liu B, Fang L, Chen J, Liu F, Wang X. miRNA-dis: microRNA precursor identification based on distance structure status pairs. *Mol BioSyst.* 2015;11:1194-1204. doi:10.1039/c5mb00050e

29. Liu B, Fang L, Liu F, Wang X, Chou K-C. iMiRNA-PseDPC: microRNA precursor identification with a pseudo distance-pair composition approach. *J Biomol Struct Dyn*. 2016;34:223-235. doi:10.1080/07391102.2015.1014422
30. Chen J, Wang X, Liu B. iMiRNA-SSF: improving the identification of microRNA precursors by combining negative sets with different distributions. *Sci Rep*. 2016;6:19062. doi:10.1038/srep19062
31. He C, Li YX, Zhang G, et al. MiRmat: mature microRNA sequence prediction. *PLoS One*. 2012;7(12):e51673. doi:10.1371/journal.pone.0051673
32. Gkirtzou K, Tsamardinos I, Tsakalides P, Poirazi P. Mature-Bayes: a probabilistic algorithm for identifying the mature miRNA within novel precursors. *PLoS One*. 2010;5(8):e11843. doi:10.1371/journal.pone.0011843
33. Leclercq M, Diallo AB, Blanchette M. Computational prediction of the localization of microRNAs within their pre-miRNA. *Nucleic Acids Res*. 2013;41:7200-7211. doi:10.1093/nar/gkt466
34. Pearson WR, Lipman DJ. Improved tools for biological sequence comparison. *Proc Natl Acad Sci USA*. 1988;85:2444-2448. doi:10.1073/pnas.85.8.2444
35. Camacho C, Coulouris G, Avagyan V, et al. BLAST+: architecture and applications. *BMC Bioinformatics*. 2009;10:421. doi:10.1186/1471-2105-10-421
36. Paraskevopoulou MD, Georgakilas G, Kostoulas N, et al. DIANA-microT web server v5.0: service integration into miRNA functional analysis workflows. *Nucleic Acids Res*. 2013;41:W169-W173. doi:10.1093/nar/gkt393
37. Liu W, Wang X. Prediction of functional microRNA targets by integrative modeling of microRNA binding and target expression data. *Genome Biol*. 2019;20:18. doi:10.1186/s13059-019-1629-z
38. Giurgiu M, Reinhard J, Brauner B, et al. CORUM: the comprehensive resource of mammalian protein complexes-2019. *Nucleic Acids Res*. 2019;47:D559-D563. doi:10.1093/nar/gky973
39. Dai X, Cheng H, Bai Z, Li J. Breast cancer cell line classification and its relevance with breast tumor subtyping. *J Cancer*. 2017;8:3131-3141. doi:10.7150/jca.18457
40. Green M, Sambrook J. *Molecular Cloning: A Laboratory Manual*. 4th ed. Cold Spring Harbor Laboratory Press; 2012. <http://molecularcloning.com/>
41. Pfaffl MW. A new mathematical model for relative quantification in real-time RT-PCR. *Nucleic Acids Res*. 2001;29:e45. doi:10.1093/nar/29.9.e45
42. Riss T, Moravec R, Niles A. Cell viability assays. In: Markossian S, Grossman A, Brimacombe K, et al., eds. *Assay Guidance Manual*. Bethesda (MD), USA: Eli Lilly & Company and the National Center for Advancing Translational Sciences; 2013. <https://www.ncbi.nlm.nih.gov/books/NBK144065/?report=classic>
43. Christofi T, Zaravinos A. RNA editing in the forefront of epitranscriptomics and human health. *J Transl Med*. 2019;17:319. doi:10.1186/s12967-019-2071-4
44. Sharma PM, Bowman M, Madden SL, Rauscher FJ, Sukumar S. RNA editing in the Wilms' tumor susceptibility gene, WT1. *Genes Dev*. 1994;8:720-731. doi:10.1101/gad.8.6.720
45. Pawlowski J, Kraft AS. Bax-induced apoptotic cell death. *Proc Natl Acad Sci USA*. 2000;97:529-531. doi:10.1073/pnas.97.2.529
46. Radu A, Neubauer V, Akagi T, Hanafusa H, Georgescu M-M. PTEN induces cell cycle arrest by decreasing the level and nuclear localization of cyclin D1. *Mol Cell Biol*. 2003;23:6139-6149. doi:10.1128/MCB.23.17.6139-6149.2003
47. Nafissi N, Khayamzadeh M, Zeinali Z, Pazooki D, Hosseini M, Akbari ME. Epidemiology and Histopathology of Breast Cancer in Iran versus Other Middle Eastern Countries. *Middle East J Cancer*. 2018;9(3):243-251. [https://mejcs.ums.ac.ir/issue\\_4948\\_4951.html](https://mejcs.ums.ac.ir/issue_4948_4951.html)
48. Gharbi S, Shamsara M, Khateri S, et al. Identification of reliable reference genes for quantification of microRNAs in serum samples of sulfur mustard-exposed veterans. *Cell journal*. 2015;17:494-501. doi:10.22074/cellj.2015.9
49. Gomes CPC, Cho J-H, Hood L, Franco OL, Pereira RW, Wang K. A review of computational tools in microRNA discovery. *Front Genet*. 2013;4:81. doi:10.3389/fgene.2013.00081
50. Liu B, Shyr Y, Cai J, Liu Q. Interplay between miRNAs and host genes and their role in cancer. *Briefings Funct Genomics*. 2018;18:255-266. doi:10.1093/bfpg/ez002
51. Li E-q, Zhang J-l. Essential role of SH3GL1 in interleukin-6(IL-6)- and vascular endothelial growth factor (VEGF)-triggered p130cas-mediated proliferation and migration of osteosarcoma cells. *Hum Cell*. 2017;30:300-310. doi:10.1007/s13577-017-0178-6
52. Tian, J, Li J, Bie B, et al. MiR-3663-3p participates in the anti-hepatocellular carcinoma proliferation activity of baicalein by targeting SH3GL1 and negatively regulating EGFR/ERK/NF- $\kappa$ B signaling. *Toxicol Appl Pharmacol*. 2021;420:115522. doi:10.1016/j.taap.2021.115522
53. Brady HJM, Gil-Gómez G. Molecules in focus Bax. The proapoptotic Bcl-2 family member, Bax. *Int J Biochem Cell Biol*. 1998;30:647-650. doi:10.1016/S1357-2725(98)00006-5
54. Pastorino JG, Chen ST, Tafani M, Snyder JW, Farber JL. The overexpression of Bax produces cell death upon induction of the mitochondrial permeability transition. *J Biol Chem*. 1998;273:7770-7775. doi:10.1074/jbc.273.13.7770
55. Weng L, Brown J, Eng C. PTEN induces apoptosis and cell cycle arrest through phosphoinositol-3-kinase/Akt-dependent and -independent pathways. *Hum Mol Gen*. 2001;10:237-242. doi:10.1093/hmg/10.3.237
56. Li X, Lin G, Wu B, Zhou X, Zhou K. Overexpression of PTEN induces cell growth arrest and apoptosis in human breast cancer ZR-75-1 cells. *Acta Biochim Biophys Sin (Shanghai)*. 2007;39:745-750. doi:10.1111/j.1745-7270.2007.00337.x
57. Rahimi A, Sedighi R, Emadi-Baygi M, et al. Bioinformatics prediction and experimental validation of a novel microRNA: hsa-miR-B43 within human CDH4 gene with a potential metastasis-related function in breast cancer. *J Cell Biochem*. 2020;121(2):1307-1316. doi:10.1002/jcb.29367
58. Stemmler MP, Hecht A, Kemler R. E-cadherin intron 2 contains cis-regulatory elements essential for gene expression. *Development*. 2005;132:965-976. doi:10.1242/dev.01662
59. Pinheiro H, Carvalho J, Oliveira P, et al. Transcription initiation arising from E-cadherin/CDH1 intron2: a novel protein isoform that increases gastric cancer cell invasion and angiogenesis. *Hum Mol Genet*. 2012;21:4253-4269. doi:10.1093/hmg/dds248
60. Tedaldi G, Molinari C, São José C, et al. Genetic and epigenetic alterations of CDH1 regulatory regions in hereditary and

- sporadic gastric cancer. *Pharmaceuticals (Basel, Switzerland)*. 2021;14:457. doi:10.3390/ph14050457
61. Piezzo M, Cocco S, Caputo R, et al. Targeting cell cycle in breast cancer: CDK4/6 inhibitors. *Int J Mol Sci*. 2020;21(18):6479. doi:10.3390/ijms21186479
  62. Sheppard KE, Pearson RB, Hannan RD. Unexpected role of CDK4 in a G2/M checkpoint. *Cell cycle (Georgetown, Tex.)*. 2015;14:1351-1352. doi:10.1080/15384101.2015.1022060
  63. Chang F, Lee JT, Navolanic PM, et al. Involvement of PI3K/Akt pathway in cell cycle progression, apoptosis, and neoplastic transformation: a target for cancer chemotherapy. *Leukemia*. 2003;17:590-603. doi:10.1038/sj.leu.2402824
  64. Zou H, Li Y, Liu X, Wang X. An APAF-1-Cytochrome c multimeric complex is a functional apoptosome that activates procaspase-9. *J Biol Chem*. 1999;274:11549-11556. doi:10.1074/jbc.274.17.11549
  65. Garrido C, Galluzzi L, Brunet M, Puig PE, Didelot C, Kroemer G. Mechanisms of cytochrome c release from mitochondria. *Cell Death Differ*. 2006;13:1423-1433. doi:10.1038/sj.cdd.4401950
  66. Bao Q, Shi Y. Apoptosome: a platform for the activation of initiator caspases. *Cell Death Differ*. 2007;14:56-65. doi:10.1038/sj.cdd.4402028
  67. Qian, B, Katsaros D, Lu L, et al. High miR-21 expression in breast cancer associated with poor disease-free survival in early stage disease and high TGF- $\beta$ 1. *Breast Cancer Res Treat*. 2009;117(1):131-140. doi:10.1007/s10549-008-0219-7
  68. Wang, H, Tan Z, Hu H, et al. microRNA-21 promotes breast cancer proliferation and metastasis by targeting LZTFL1. *BMC Cancer*. 2019;19(1):1-13. doi:10.1186/s12885-019-5951-3
  69. Nouraei N, Van Roosbroeck K, Vasei M, et al. Expression, tissue distribution and function of miR-21 in esophageal squamous cell carcinoma. *PLoS One*. 2013;8(9):e73009. doi:10.1371/journal.pone.0073009
  70. Bade LK, Goldberg JE, DeHut HA, Hall MK, Schwertfeger KL. Mammary tumorigenesis induced by fibroblast growth factor receptor 1 requires activation of the epidermal growth factor receptor. *J Cell Sci*. 2011;124:3106-3117. doi:10.1242/jcs.082651
  71. Pang, M-F, Georgoudaki AM, Lambut L, et al. TGF- $\beta$ 1-induced EMT promotes targeted migration of breast cancer cells through the lymphatic system by the activation of CCR7/CCL21-mediated chemotaxis. *Oncogene*. 2016;35:748-760. doi:10.1038/onc.2015.133
  72. Slattery ML, Lundgreen A, John EM, et al. MAPK genes interact with diet and lifestyle factors to alter risk of breast cancer: the Breast Cancer Health Disparities Study. *Nutr Cancer*. 2015;67:292-304. doi:10.1080/01635581.2015.990568
  73. Vora, SR, Juric D, Kim N, et al. CDK 4/6 inhibitors sensitize PIK3CA mutant breast cancer to PI3K inhibitors. *Cancer Cell*. 2014;26:136-149. doi:10.1016/j.ccr.2014.05.020
  74. ShahidSales S, Mehramiz M, Ghasemi F, et al. A genetic variant in CDKN2A/B gene is associated with the increased risk of breast cancer. *J Clin Lab Anal*. 2018;32:e22190. doi:10.1002/jcla.22190
  75. Asada K, Miyamoto K, Fukutomi T, et al. Reduced expression of GNA11 and silencing of MCT1 in human breast cancers. *Oncology*. 2003;64:380-388. doi:10.1159/000070297
  76. Zou T, Liu J, She L, et al. A perspective profile of ADCY1 in cAMP signaling with drug-resistance in lung cancer. *J Cancer*. 2019;10:6848-6857. doi:10.7150/jca.36614
  77. de Groot JS, Ratze MA, van Amersfoort M, et al.  $\alpha$ E-catenin is a candidate tumor suppressor for the development of E-cadherin-expressing lobular-type breast cancer. *J Pathol*. 2018;245:456-467. doi:10.1002/path.5099
  78. Huang P, Chen A, He W, et al. BMP-2 induces EMT and breast cancer stemness through Rb and CD44. *Cell Death Discov*. 2017;3:17039. doi:10.1038/cddiscovery.2017.39
  79. Simmons GE, Pandey S, Nedeljkovic-Kurepa A, Saxena M, Wang A, Pruitt K. Frizzled 7 expression is positively regulated by SIRT1 and  $\beta$ -catenin in breast cancer cells. *PLoS One*. 2014;9:e98861. doi:10.1371/journal.pone.0098861

## SUPPORTING INFORMATION

Additional supporting information may be found in the online version of the article at the publisher's website.

**How to cite this article:** Gharbi S, Mohammadi Z, Dezaki MS, Dokanehiifard S, Dabiri S, Korsching E. Characterization of the first microRNA in human *CDH1* that affects cell cycle and apoptosis and indicates breast cancers progression. *J Cell Biochem*. 2022;1-16. doi:10.1002/jcb.30211